

## Chiral mirrors

Eric Plum<sup>1,a)</sup> and Nikolay I. Zheludev<sup>1,2,b)</sup>

<sup>1</sup>Optoelectronics Research Centre and Centre for Photonic Metamaterials, University of Southampton, Highfield, Southampton SO17 1BJ, United Kingdom

<sup>2</sup>The Photonics Institute and Centre for Disruptive Photonic Technologies, Nanyang Technological University, Singapore 637378, Singapore

(Received 27 March 2015; accepted 21 May 2015; published online 1 June 2015)

Mirrors are used in telescopes, microscopes, photo cameras, lasers, satellite dishes, and everywhere else, where redirection of electromagnetic radiation is required making them arguably the most important optical component. While conventional isotropic mirrors will reflect linear polarizations without change, the handedness of circularly polarized waves is reversed upon reflection. Here, we demonstrate a type of mirror reflecting one circular polarization without changing its handedness, while absorbing the other. The polarization-preserving mirror consists of a planar metasurface with a subwavelength pattern that cannot be superimposed with its mirror image without being lifted out of its plane, and a conventional mirror spaced by a fraction of the wavelength from the metasurface. Such mirrors enable circularly polarized lasers and Fabry-Pérot cavities with enhanced tunability, gyroscopic applications, polarization-sensitive detectors of electromagnetic waves, and can be used to enhance spectroscopies of chiral media. © 2015 AIP Publishing LLC.

[<http://dx.doi.org/10.1063/1.4921969>]

Conventional mirrors, from polished obsidian surfaces used in Anatolia 8000 years ago<sup>1</sup> to metallic mirrors, interference-based dielectric multilayers, Bragg reflectors and Faraday rotator mirrors<sup>2</sup> used today are isotropic and share the property that they will reverse the handedness of circularly polarized electromagnetic waves upon reflection, see Fig. 1(a). Metallic surfaces are also known as “electric mirrors” as they reverse the direction of the reflected electromagnetic wave’s electric field, while metamaterial-based isotropic “magnetic mirrors,” which reverse the wave’s magnetic field upon reflection, have also been reported.<sup>3–7</sup> Combining both concepts, anisotropic handedness-preserving mirrors have been introduced,<sup>8</sup> see Fig. 1(b). Such structures avoid the handedness reversal by reflecting their perpendicular linear eigenpolarizations with a phase difference of  $\pi$ , i.e., they are an electric mirror for one eigenpolarization and a magnetic mirror for the other. Furthermore, polarization insensitive and linear polarization perfect absorbers consisting of a metasurface with a backing conventional mirror,<sup>8–13</sup> or a pair of metasurfaces,<sup>14</sup> separated by a lossy dielectric spacer have been demonstrated, see Fig. 1(c), and some anisotropic realizations have been shown to act as magnetic mirror for one linear polarization.<sup>8,9</sup>

Here, we demonstrate a type of mirror, which reflects one circular polarization without polarization change, while absorbing the other, e.g., a handedness-preserving mirror for right-handed circularly polarized waves (RCP, +) that is a perfect absorber for left-handed circular polarization (LCP, –), or vice versa, see Figs. 1(d) and 1(e).

Key for the realization of such polarization selective RCP (or LCP) mirrors is a chiral structure to enable different responses to electromagnetic waves of opposite handedness.

In principle, conventional 3D-chiral<sup>15</sup> media and the associated effect of circular dichroism (optical activity)<sup>16</sup> lead to different losses for waves of opposite handedness. However, for a reflecting device, the handedness reversal of the wave upon reflection would undo any discrimination between RCP and LCP during the second pass through the 3D-chiral

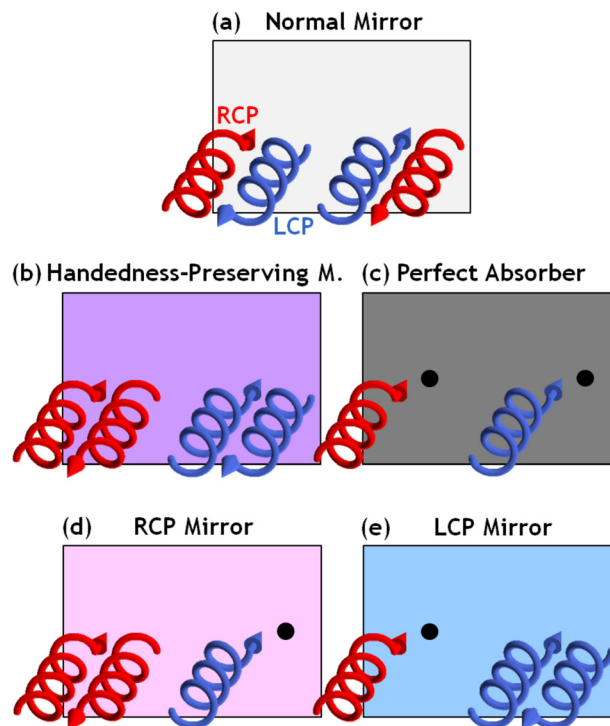


FIG. 1. Mirrors. (a) A conventional mirror reverses the handedness of circularly polarized waves. (b) Structures designed to reflect  $x$  and  $y$  polarizations with a phase difference of  $\pi$  act as handedness-preserving mirrors.<sup>8</sup> (c) Perfect absorbers do not reflect. Here, we demonstrate (d) RCP and (e) LCP mirrors, which reflect circularly polarized waves of one handedness without handedness reversal, while absorbing the other.

<sup>a)</sup>Electronic mail: erp@orc.soton.ac.uk

<sup>b)</sup>Electronic mail: niz@orc.soton.ac.uk URL: [www.nanophotonics.org.uk](http://www.nanophotonics.org.uk)

medium. In fact, what is needed is a medium that reverses its response with the handedness reversal of the wave upon reflection in order to amplify the chiral polarization selectivity, rather than eliminating it. This peculiar property is associated with 2D (planar) chiral materials.<sup>17,18</sup> In contrast to a 3D-chiral helix, which has the same sense of twist when observed from opposite ends, a flat 2D-chiral spiral reverses its sense of twist for observation from opposite sides. The same is true for any pattern that cannot be superimposed with its mirror image without being lifted out of its plane and such patterns are said to be 2D-chiral. Lossy, anisotropic, 2D-chiral metasurfaces exhibit a corresponding optical effect, where the same circularly polarized wave will be transmitted and absorbed differently when illuminating opposite sides of the metasurface.<sup>19–27</sup> In particular, such 2D-chiral metasurfaces predominantly absorb RCP incident on one side and LCP incident on the opposite side. We note that also the Faraday effect enables differential absorption of circularly polarized waves, which would aggregate during both passes through the Faraday medium, however, such a “Faraday absorber mirror” would still reverse the handedness of the reflected wave.<sup>2</sup> In

contrast, the 2D-chiral effect leads to circular polarization conversion enabling it to undo the handedness reversal of the wave upon reflection. Thus, optical properties of 2D-chiral materials are exactly what is needed to make a device that absorbs one incident circular polarization, while reflecting the other without polarization change. Therefore, we construct the handedness-preserving mirror/perfect absorber by placing a 2D-chiral metasurface in front of a conventional mirror.

Fig. 2 shows proof-of-principle experiments at microwave frequencies between 4.5 and 6.5 GHz (67–46 mm wavelength) performed in an anechoic chamber using broadband microwave antennas (Schwarzbeck BBHA 9120D) equipped with collimating lenses and a vector network analyzer (Agilent E8364B). As illustrated by Fig. 2(a), a conventional metal mirror simply converts RCP to LCP ( $R_{-+}$ ) and LCP to RCP ( $R_{+-}$ ) with 100% efficiency. Here,  $R_{ij}$  are the reflection coefficients for circularly polarized waves in terms of intensity, and RCP is defined as clockwise rotation of the electric field vector at a fixed point as seen by an observer looking into the beam. These reflection characteristics change dramatically when an achiral split ring metasurface is

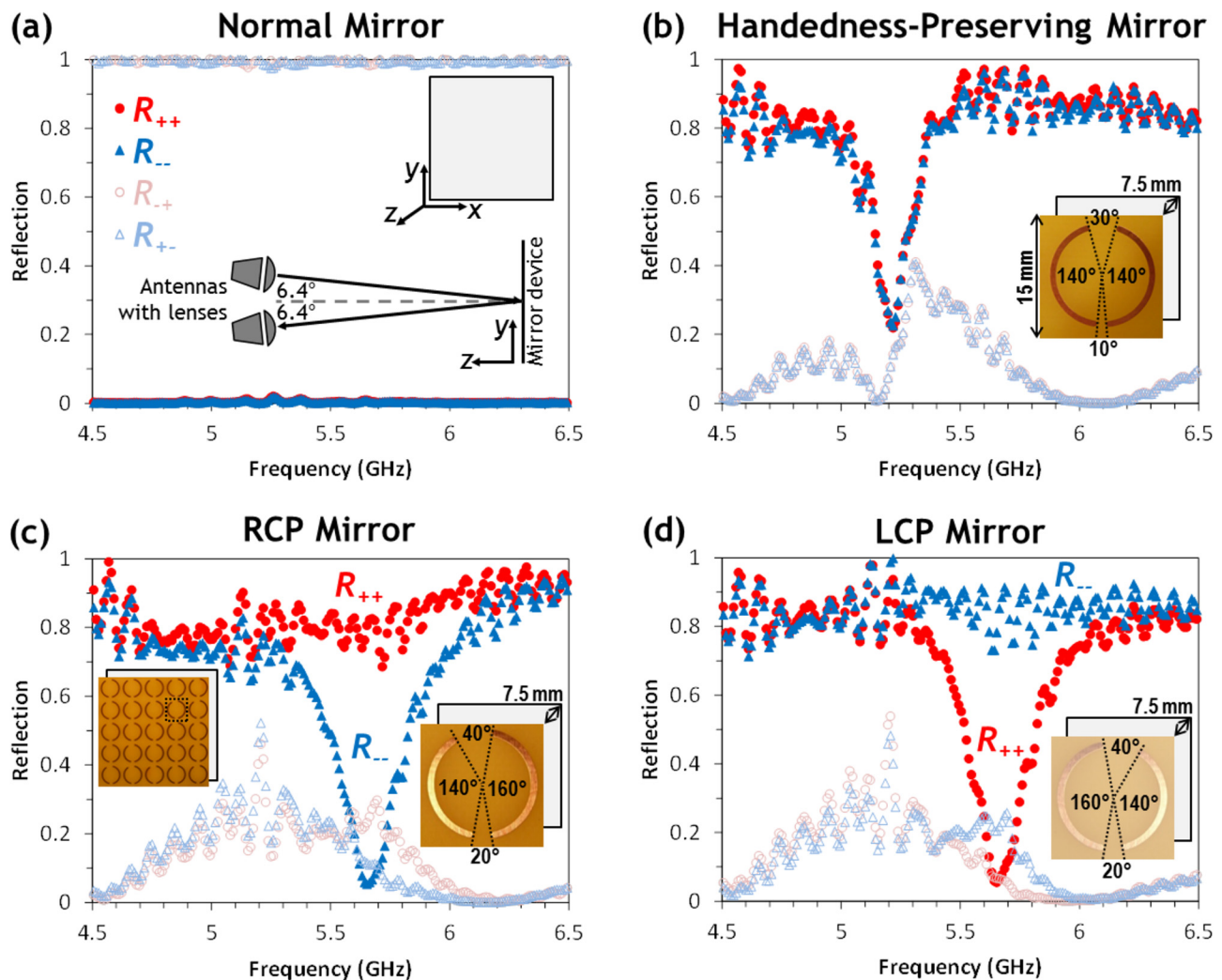


FIG. 2. Reflection spectra of achiral and chiral mirrors. (a) Conventional mirror consisting of an aluminum plate. (b) Handedness-preserving, (c) RCP, and (d) LCP mirrors consisting of metamaterial arrays of (b) achiral and ((c) and (d)) 2D-chiral split rings placed 7.5 mm in front of an aluminum plate. Insets show a unit cell of the respective mirror structure, the experimental setup and a fragment of the RCP mirror. All structures have a diameter of 220 mm and the metasurfaces consist of a square array of about 170 copper split rings (radius 6 mm, line width 0.8 mm, period 15 mm) supported by a lossy dielectric substrate of about 1.5 mm thickness.

placed in front of the metal mirror, see Fig. 2(b), where the periodic metasurface is represented by a single unit cell. The achiral and anisotropic composite structure reflects circularly polarized waves without polarization change ( $R_{++}$ ,  $R_{--}$ ) with 80%–90% efficiency, except for an absorption resonance around 5.2 GHz. Thus, we demonstrate a metadvice that can act both as low-loss handedness-preserving mirror and (almost) perfect absorber. Fig. 2(c) shows what happens, when we introduce 2D-chiral symmetry breaking. When both wires and gaps of the split ring have different sizes, the pattern loses its line of mirror symmetry, i.e., it becomes different from its mirror image and therefore 2D-chiral. This is apparent from its electromagnetic response, which becomes different for incident waves of opposite handedness. At 5.65 GHz, the 2D-chiral mirror has an absorption resonance for LCP ( $R_{--}$ ), while the handedness-preserving reflectivity for RCP ( $R_{++}$ ) remains high. This RCP mirror turns into an LCP mirror, when the handedness of the metasurface is reversed by flipping it over so that the split rings (rather than the substrate) face the metal mirror, see Fig. 2(d).

In order to understand the response of the composite structure, it is useful to consider the properties of metasurfaces without the backing mirror first. For a single illuminating beam, absorption in metasurfaces cannot exceed 50%, limiting the absorption contrast  $A_- - A_+$  of a 2D-chiral metasurface to 50%. As metasurfaces scatter equally in the

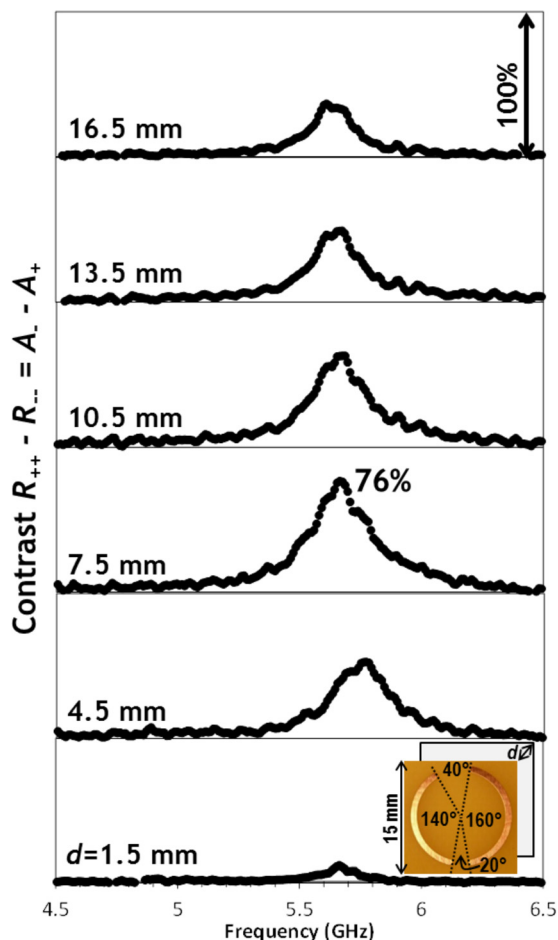


FIG. 3. Polarization contrast of an RCP mirror as a function of the spacing  $d$  between split rings and aluminum plate.

transmission and reflection directions, the corresponding limit for the reflectivity contrast  $R_{++} - R_{--}$  is 25% (Ref. 28). However, it has recently been demonstrated that absorption in metasurfaces can approach 100% for in-phase coherent illumination from opposite sides.<sup>29</sup> In our case, the incident wave and (multiple) reflection(s) by the metal mirror lead to coherent illumination of front and back of our metasurfaces with a phase difference that is controlled by the metasurface-to-mirror spacing. Thus, the spacing can be adjusted to achieve in-phase excitation to maximize absorption of the resonant polarization. As illustrated by Fig. 3, resonant LCP absorption and thus the reflectivity contrast  $R_{++} - R_{--}$  are maximized by constructive interference of incident and reflected waves on the metasurface when the separation between split rings and metal mirror is 7.5 mm. At this spacing, the observed reflectivity contrast reaches 76% and we expect that values approaching 100% can be achieved through simultaneous optimization of metasurface-to-mirror spacing, substrate losses, and 2D-chiral split ring geometry. Thus, 2D-chiral mirrors as reported here can be tailored to exhibit the ultimate 2D-chiral optical effect.

In order to accurately link the reflectivity contrast  $R_{++} - R_{--}$  to absorption, the experimental results shown in Figs. 2(c) and 2(d) need to be discussed in slightly more detail. Our measurements show a small difference between  $R_{-+}$  and  $R_{+-}$ . This is circular dichroism caused by extrinsic 3D chirality<sup>30</sup> associated with a small, but non-zero, angle of incidence ( $6.4^\circ$  above the normal) that cannot be avoided in our experiments due to having to place the emitting and receiving antennas next to each other. This 3D-chiral effect occurs at oblique incidence onto metasurfaces lacking two-fold rotational symmetry and has been introduced<sup>30</sup> and extensively studied for split ring metasurfaces in Ref. 28 and references therein. It reverses for opposite angles of incidence—which has been confirmed by control experiments with the opposite angle of incidence ( $6.4^\circ$  below the normal)—and vanishes at normal incidence. Thus, at normal incidence  $R_{-+} = R_{+-}$ , and in this case, the reflectivity contrast corresponds exactly to the difference in absorption for LCP and RCP  $A_- - A_+ = R_{++} - R_{--}$ . Finally, we would like to note that a 2D-chiral meta-molecule with a backing mirror corresponds to a 3D-chiral meta-molecule of a volume metamaterial. Interpreted in this way, our results show that reflectivity from such a 3D-chiral medium is sensitive to the handedness of the polarization state.

It is interesting to consider potential applications that are enabled by the handed mirror. Most obvious uses include reflective circular polarizers, circular polarization detectors (e.g., bolometers), and self-polarizing Fabry-Pérot cavities. The latter case is illustrated by Fig. 4. The modes of conventional cavities consisting of a pair of normal isotropic mirrors require the cavity length to be a half integer multiple of the wavelength. The modes themselves are standing wave patterns with nodes and anti-nodes. In case of circular polarization, the counterpropagating RCP and LCP waves interfere forming an electric field pattern that looks like a frozen linearly polarized wave rotating around the propagation direction, see Figs. 4(a) and 4(f) (Multimedia view). The circularly polarized modes supported by cavities assembled

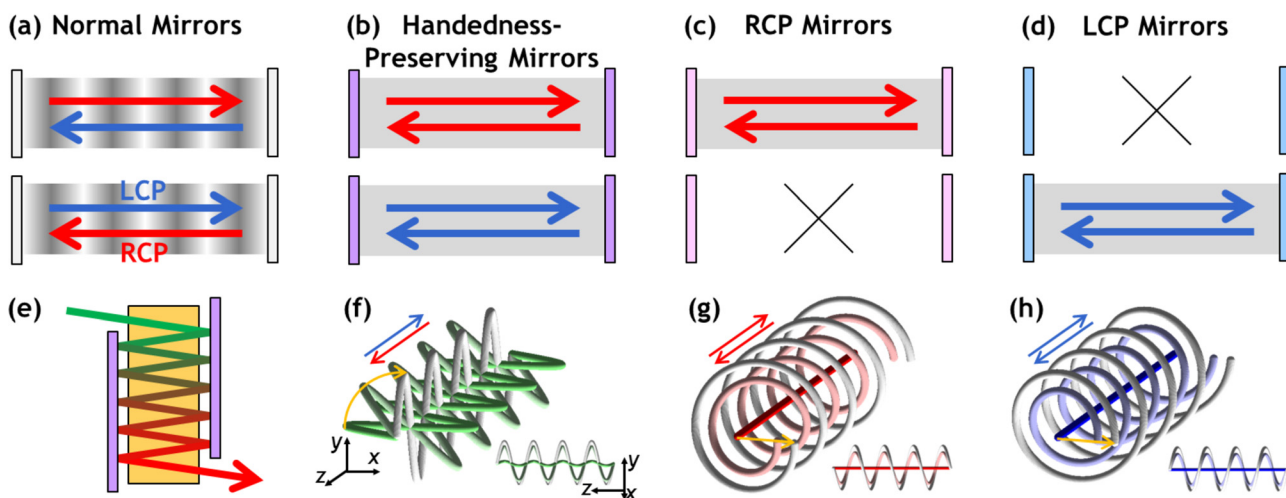


FIG. 4. Waves in cavities based on achiral and chiral mirrors. (a) Conventional Fabry-Pérot cavities can support waves of opposite handedness propagating in opposite directions, which form a standing wave with nodes. (b) Cavities based on handedness-preserving mirrors can support both RCP and LCP modes, which do not have nodes. (c) RCP and (d) LCP cavities will only support a circularly polarized mode of the given handedness. (e) Multi-pass enhancement of optical activity using handedness-preserving mirrors: The initially linear polarization state (green) rotates and becomes increasingly elliptically polarized (transition to red) with every pass of the wave through the optically active medium (yellow). (f)–(h) Standing waves of electric field formed by counterpropagating circularly polarized waves of (f) opposite handedness, as in (a); (g) equal RCP, as in (b) and (c); and (h) equal LCP, as in (b) and (d). In (f)–(h), different colors illustrate the evolution of the field pattern in time. Color changes towards white show the temporal evolution of the electric field pattern in phase steps of  $45^\circ$  as indicated by the yellow arrows. Corresponding animations showing the temporal evolution are provided. (Multimedia view) 4(f) [URL: <http://dx.doi.org/10.1063/1.4921969.1>], 4(g) [URL: <http://dx.doi.org/10.1063/1.4921969.2>], and 4(h) [URL: <http://dx.doi.org/10.1063/1.4921969.3>]

from handedness-preserving and handed mirrors are very different. These cavities support counterpropagating waves of the same handedness (Figs. 4(b)–4(d)), which has several interesting consequences. The waves in the cavity interfere forming a field structure that does not have nodes or antinodes, but the electric field distribution looks like a helix with a diameter that oscillates in time, see Figs. 4(g) and 4(h) (Multimedia view). Absence of nodes and anti-nodes removes the requirement for the cavity length to be a half integer multiple of the wavelength to support the mode. Instead, the phase relationship between waves before and after reflection is determined by the 2D-chiral mirror's azimuthal orientation. Therefore, the cavity can be matched to any chosen wavelength by either changing its length or by azimuthal rotation of one of the mirrors, where a cavity length change of half a wavelength is equivalent to a mirror rotation by  $180^\circ$ . While tuning of conventional Fabry-Pérot cavities requires fine adjustment of the mirror position within half a wavelength, a resonator with handedness-preserving mirrors can be conveniently tuned by axial rotation of the mirror within  $180^\circ$ . In contrast to cavities based on anisotropic handedness-preserving mirrors that will support modes with all sorts of polarizations, the cavities consisting of a pair of either RCP or LCP mirrors are self-polarizing, supporting only circularly polarized waves of one handedness. If combined with an isotropic gain medium, such cavities would allow the realization of easy-to-tune circularly polarized lasers based on the linear Fabry-Pérot geometry. The use of such a laser resonator without nodes of electric (magnetic) field can enhance the efficiency of laser sources by the virtue of more homogeneous utilization of gain. Such lasers will be sensitive to mirror rotation around the resonator axis and thus could be used for gyroscopic applications. Furthermore, exploiting that a medium placed in such a laser cavity will only interact

with circularly polarized waves of one handedness, such cavities could be used for resonantly enhanced high accuracy intracavity measurements of optical activity (circular birefringence and circular dichroism): Placing a 3D-chiral medium inside RCP and LCP cavities allows measurements of the induced phase shift (cavity detuning) and absorption (mode attenuation) for RCP and LCP waves independently. Moreover, similarly to how the optical Faraday effect can be enhanced by multiple passes of light bouncing between two conventional mirrors, the optical activity effect can be enhanced using the multi-pass arrangement with polarization-preserving mirrors, which can be used for enhanced detection of molecular chirality that is considered as a universal indication of life forms, see Fig. 4(e).

In summary, we demonstrate a type of mirror that is a handedness-preserving reflector for a single circular polarization and a coherent perfect absorber for circularly polarized waves of the opposite handedness. We argue that such metadevices can, in principle, approach 100% polarization contrast. Since enantiomerically sensitive 2D-chiral plasmonic metasurfaces have already been demonstrated,<sup>20</sup> we anticipate that applications from polarization control to circularly polarized detectors, cavities, and lasers as well as optical activity measurements with resonantly enhanced sensitivity in the optical part of the spectrum shall be possible.

This work was supported by the MOE Singapore (Grant No. MOE2011-T3-1-005), the Leverhulme Trust and the UK's Engineering and Physical Sciences Research Council (Grant No. EP/G060363/1). The data from this paper can be obtained from the University of Southampton e-Print research repository: <http://dx.doi.org/10.5258/SOTON/376745>.

- <sup>1</sup>J. M. Enoch, *Optometry Vision Sci.* **83**, 775 (2006).
- <sup>2</sup>M. Martinelli, *Opt. Commun.* **72**, 341 (1989).
- <sup>3</sup>D. Sievenpiper, Z. Lijun, R. F. J. Broas, N. G. Alexopolous, and E. Yablonovitch, *IEEE Trans. Microwave Theory Tech.* **47**, 2059 (1999).
- <sup>4</sup>A. P. Feresidis, G. Goussetis, S. H. Wang, and J. C. Vardaxoglou, *IEEE Trans. Antennas Propag.* **53**, 209 (2005).
- <sup>5</sup>D. J. Kern, D. H. Werner, A. Monorchio, L. Lanuzza, and M. J. Wilhelm, *IEEE Trans. Antennas Propag.* **53**, 8 (2005).
- <sup>6</sup>H. Rostami, Y. Abdi, and E. Arzi, *Carbon* **48**, 3659 (2010).
- <sup>7</sup>S. Liu, M. B. Sinclair, T. S. Mahony, Y. C. Jun, S. Campione, J. Ginn, D. A. Bender, J. R. Wendt, J. F. Ihlefeld, P. G. Clem *et al.*, *Optica* **1**, 250 (2014).
- <sup>8</sup>V. A. Fedotov, S. L. Prosvirnin, A. V. Rogacheva, and N. I. Zheludev, *Appl. Phys. Lett.* **88**, 091119 (2006).
- <sup>9</sup>V. A. Fedotov, P. L. Mladyonov, S. L. Prosvirnin, and N. I. Zheludev, *Phys. Rev. E* **72**, 056613 (2005).
- <sup>10</sup>B. Zhang, Y. Zhao, Q. Hao, B. Kiraly, I.-C. Khoo, S. Chen, and T. J. Huang, *Opt. Express* **19**, 15221 (2011).
- <sup>11</sup>Q. Feng, M. Pu, C. Hu, and X. Luo, *Opt. Lett.* **37**, 2133 (2012).
- <sup>12</sup>G. Dayal and S. A. Ramakrishna, *Opt. Express* **20**, 17503 (2012).
- <sup>13</sup>D. Shrekenhamer, W.-C. Chen, and W. J. Padilla, *Phys. Rev. Lett.* **110**, 177403 (2013).
- <sup>14</sup>N. I. Landy, S. Sajuyigbe, J. J. Mock, D. R. Smith, and W. J. Padilla, *Phys. Rev. Lett.* **100**, 207402 (2008).
- <sup>15</sup>L. Kelvin, *Baltimore Lectures on Molecular Dynamics and the Wave Theory of Light* (C. J. Clay and Sons, Cambridge University Press Warehouse, London, 1904), p. 619.
- <sup>16</sup>F. J. D. Arago, *Mémoires de la classe des sciences math. et phys. de l'Institut Impérial de France* (1812), p. 93.
- <sup>17</sup>L. Hecht and L. Barron, *Chem. Phys. Lett.* **225**, 525 (1994).
- <sup>18</sup>L. R. Arnaut and L. E. Davis, in *Proceedings of the International Conference on Electromagnetics in Advanced Applications* (Nexus Media, Swanley, UK, 1995), pp. 381–388.
- <sup>19</sup>V. A. Fedotov, P. L. Mladyonov, S. L. Prosvirnin, A. Rogacheva, Y. Chen, and N. I. Zheludev, *Phys. Rev. Lett.* **97**, 167401 (2006).
- <sup>20</sup>V. A. Fedotov, A. S. Schwanecke, N. I. Zheludev, V. V. Khardikov, and S. L. Prosvirnin, *Nano Lett.* **7**, 1996 (2007).
- <sup>21</sup>A. Drezet, C. Genet, J.-Y. Laluet, and T. W. Ebbesen, *Opt. Express* **16**, 12559 (2008).
- <sup>22</sup>E. Plum, V. A. Fedotov, and N. I. Zheludev, *Appl. Phys. Lett.* **94**, 131901 (2009).
- <sup>23</sup>S. V. Zhukovsky, A. V. Novitsky, and V. M. Galynsky, *Opt. Lett.* **34**, 1988 (2009).
- <sup>24</sup>E. Plum, V. A. Fedotov, and N. I. Zheludev, *J. Opt.* **13**, 024006 (2011).
- <sup>25</sup>A. V. Novitsky, V. M. Galynsky, and S. V. Zhukovsky, *Phys. Rev. B* **86**, 075138 (2012).
- <sup>26</sup>Z. Li, M. Gokkavas, and E. Ozbay, *Adv. Opt. Mater.* **1**, 482 (2013).
- <sup>27</sup>L. Wu, Z. Yang, Y. Cheng, M. Zhao, R. Gong, Y. Zheng, J. Duan, and X. Yuan, *Appl. Phys. Lett.* **103**, 021903 (2013).
- <sup>28</sup>E. Plum, Ph.D. dissertation, University of Southampton, 2010.
- <sup>29</sup>J. Zhang, K. F. MacDonald, and N. I. Zheludev, *Light: Sci. Appl.* **1**, e18 (2012).
- <sup>30</sup>E. Plum, V. A. Fedotov, and N. I. Zheludev, *Appl. Phys. Lett.* **93**, 191911 (2008).